Supporting Information

Structural and Electrochemical Properties of Li ion Solvation Complexes in the Salt-Concentrated Electrolytes Using an Aprotic Donor Solvent, *N*,*N*-Dimethylformamide

Kenta Fujii,* *Hideaki Wakamatsu, Yanko Todorov, Nobuko Yoshimoto, and Masayuki Morita*.

Graduate School of Sciences and Technology for Innovation, Yamaguchi University, 2-16-1 Tokiwadai, Ube, Yamaguchi 755-8611.

KEYWORDS. Li salt-concentrated electrolytes, Li^+ ion complexes, *N*,*N*-dimethylformamide (DMF), Li^+ ion batteries.

Distribution of TFSA species from Raman data. Total concentration of TFSA anions, c_T, in LiTFSA/DMF solutions is given by the equation, $c_T = c_f + c_b$, where c_f and c_b are the free and bound TFSA anions. The integrated intensity of the free TFSA is given by $I_f = J_f c_f$. Here, note that no coordination of TFSA anions occurs at low LiTFSA concentrations (c_{Li}<2.0 mol dm^{-3}); Li^+ ions are solvated only by DMF molecules, meaning that all of the TFSA anions exist as a free TFSA in the bulk and $c_{Li} = c_f$. Thus, the slope of the I_f vs. c_{Li} shown blow figure corresponds to the $J_{f\,(TFSA)}$ value (= 0.66) in this system and then we can experimentally estimate the c_f value in a given c_{Li} solutions. In the c_{Li} range 2.0–2.5 mol dm^{-3}, the TFSA anions coordinate with Li^+ ions in a monodentate manner, not in a bidentate one. The c_T is thus represented by $c_T = c_f + c_{b\,(mono)}$ in this c_{Li} range where $c_{b\,(mono)}$ is the monodentate bound TFSA. As the result, the $c_{b\,(mono)}$ (= $c_T - c_f$) can be determined and the $J_{b\,(mono)}$ can be also determined using the relationship of $I_{b\,(mono)} = J_{b\,(mono)} c_{b\,(mono)}$ where $I_{b\,(mono)}$ is the integrated intensity of bound mono-TFSA observed at 747.3 cm^{-1}. Finally, the concentration of bound TFSA with bidentate manner, $c_{b\,(bi)}$, in the solutions with c_{Li} > 2.5 mol dm^{-3}, is obtained as follows; $c_{b\,(bi)} = c_T - c_f - c_{b\,(mono)}$. The distribution functions of free, mono-, and bi-TFSA species in the solutions are thus calculated by c_f/c_T, $c_{b\,(mono)}/c_T$, and $c_{b\,(bi)}/c_T$, respectively. The $J_{b\,(mono)}$ and $J_{b\,(bi)}$ values oobtained here were 0.65 and 0.72, respectively.

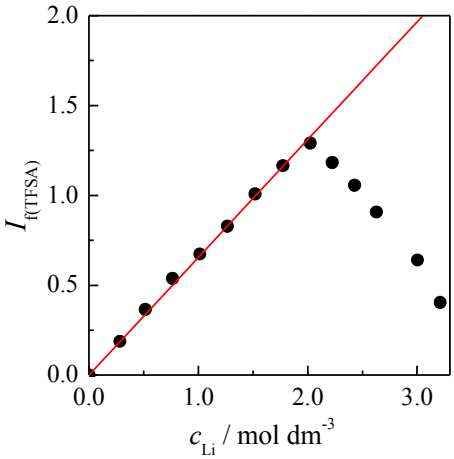

Table S1. Molar concentration (c_{Li}), mole fraction (x_{Li}), and density (d) values of LiTFSA in DMF solutions.

c_{Li} / mol dm^{-3}	x_{Li}	d / g cm^{-3}
0	0	0.9445
0.28	0.02	0.9877
0.52	0.04	1.0232
0.77	0.06	1.0611
1.01	0.08	1.0985
1.27	0.11	1.1376
1.52	0.13	1.1775
1.77	0.16	1.2150
2.02	0.18	1.2527
2.22	0.20	1.2825
2.43	0.22	1.3123
2.63	0.25	1.3433
3.00	0.29	1.3947
3.21	0.32	1.4251

Table S2. HOMO and LUMO energy levels, and binding energies (ΔE_{bind}) of the isolated DMF and TFSA anions (cis and trans conformers) and the Li^+ ion complexes with various coordination structures (shown in Figure S2). The parentheses (DMF or TFSA) indicate the species where the HOMO or LUMO appears.

	HOMO / eV	LUMO / eV	ΔE_{bind} [a] / kJ mol^{-1}
DMF	−6.96	−0.16	
cis-TFSA	−0.16	0.11	
trans-TFSA	−0.16	0.11	
1a	−9.58	−2.70	−543.23
1b	−5.79	−1.66	−740.87
1c	−7.20 (DMF)	−0.62 (DMF)	−761.71
1d	−7.57 (DMF)	−0.79 (DMF)	−726.66
1e	−4.91 (DMF)	1.24 (DMF)	−786.18
1f	−5.18 (DMF)	1.31 (DMF)	−761.46
1g	−3.07 (DMF)	3.07 (DMF)	−622.22
2a	−10.31 (DMF)	−3.35 (TFSA)	−1072.04
2b	−9.97 (DMF)	−3.60 (TFSA)	−1039.61
2c	−9.95 (DMF)	−3.88 (TFSA)	−1007.89
2d	−9.56 (DMF)	−3.37 (TFSA)	−1100.77
2e	−9.64 (DMF)	−3.06 (DMF)	−1169.40
2f	−9.75 (DMF)	−3.03 (DMF)	−1149.85
2g	−9.48 (DMF)	−2.69 (DMF)	−1237.64

[a] The ΔE_{bind} for the $[Li_x(DMF)_n(TFSA)_m]$ was calculated as the SCF energy difference between the optimized complex and single components (Li^+, DMF and $TFSA^-$) according to $\Delta E_{bind} = E_{SCF}(\text{complex}) - xE_{SCF}(Li^+) - nE_{SCF}(\text{DMF}) - mE_{SCF}(\text{TFSA})$, and then corrected by basis set superposition error (BSSE) using the counterpoise method.

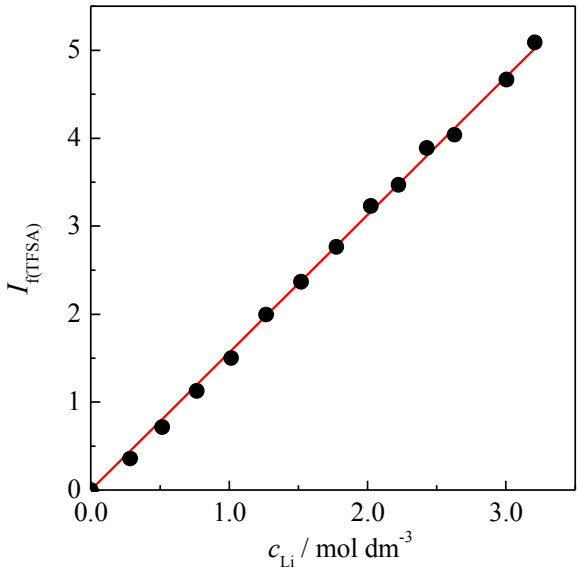

Figure S1. Raman intensities at 1339.0 cm^{-1}, which is attributed to TFSA, plotted against c_{Li}. The 1339.0 cm^{-1} band linearly increases with increasing c_{Li}, irrespective of coordination to Li ion and thus was used as an internal standard in normalization of the observed Raman spectra.

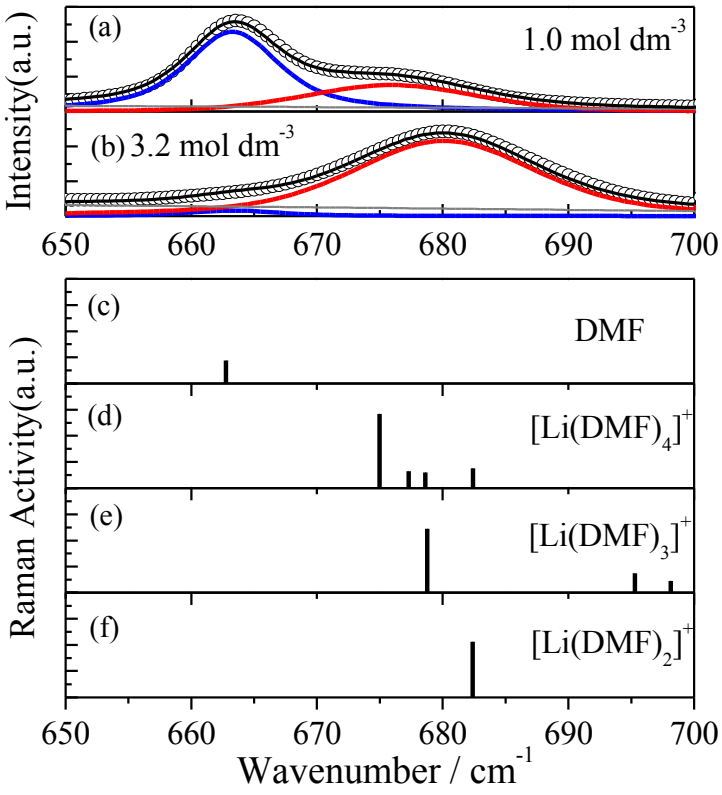

Figure S2. The observed Raman spectra for (a) 1.0 and (b) 3.2 mol dm^{-3} LiTFSA/DMF solutions and the theoretical Raman bands calculated for (c) isolated DMF, (d) $[Li(DMF)_4]^+$, (e) $[Li(DMF)_3]^+$, and (f) $[Li(DMF)_2]^+$ complexes by DFT calculations.

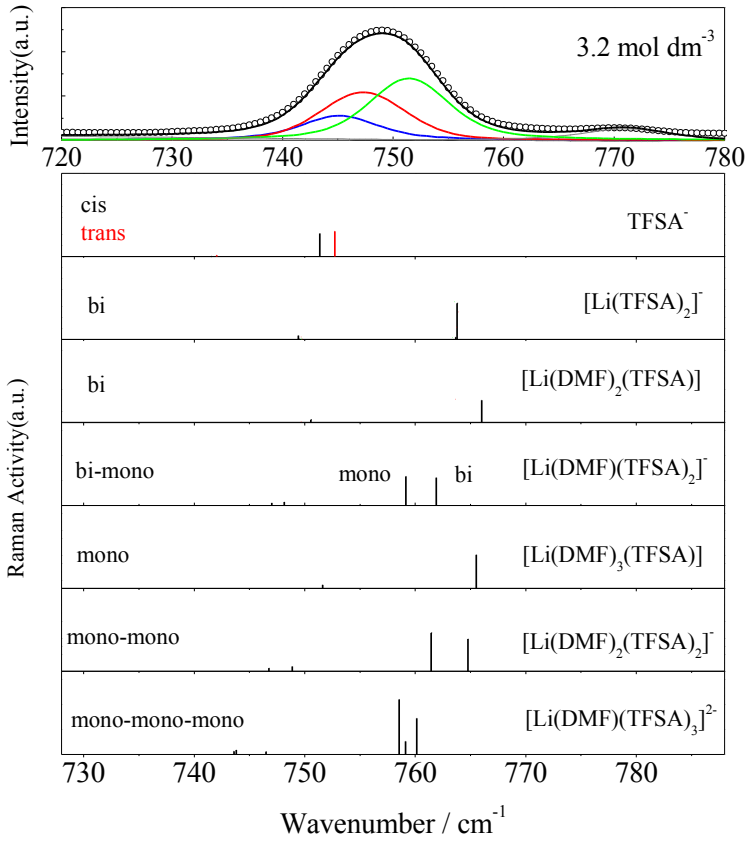

Figure S3. The theoretical Raman bands calculated for $[Li(DMF)_n(TFSA)_m]$ complexes by DFT calculations, together with the observed spectrum for LiTFSA/DMF solution with c_{Li} = 3.2 mol dm^{-3}.

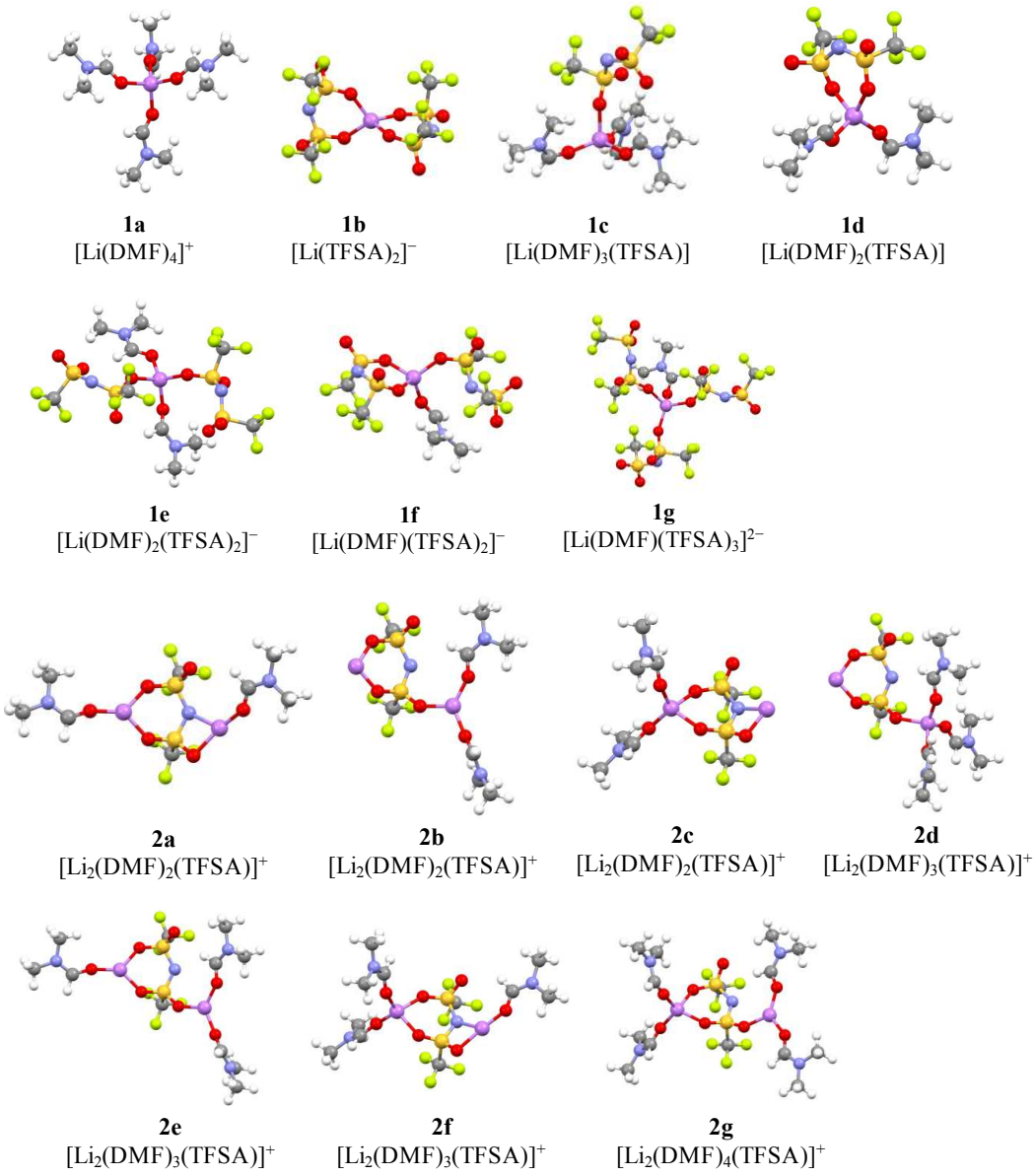

Figure S4. The optimized geometries of mononuclear (**1a**–**g**) and binuclear (**2a**–**g**) Li-ion complexes by DFT calculations.

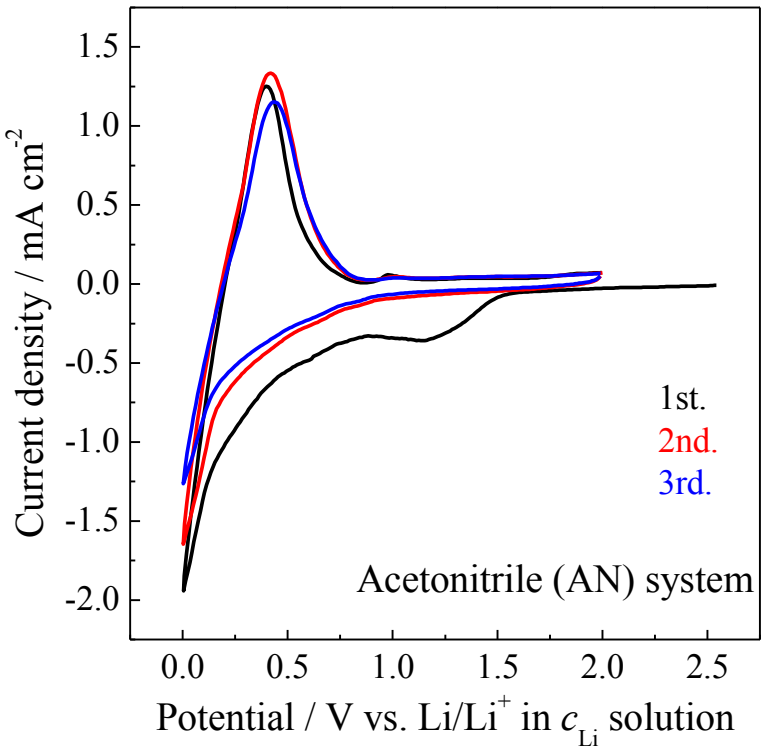

Figure S5. CV profiles for graphite electrode in LiTFSA/acetonitrile electrolyte solution (c_{Li} = 3.7 mol dm^{-3}).